Open Access

Recent Progress in Materials

LIDSEN Publishing Inc.

Original Research

Behavior of RC Buildings under Blast Loading: Case Study

Fathi M. Layas [1], Vail Karakale [2,*], Ramadan E. Suleiman [1]

1. Department of Civil Engineering, Faculty of Engineering, University of Benghazi, Benghazi, Libya; E-Mails: fmlayas@yahoo.com, resuleiman@yahoo.com
2. Department of Civil Engineering, Faculty of Engineering and Natural Sciences, Istanbul Medeniyet University, Istanbul, Turkey; E-Mail: vail.karakale@medeniyet.edu.tr

* **Correspondence:** Vail Karakale; E-Mail: vail.karakale@medeniyet.edu.tr

Academic Editor: Mostafa Seifan

Special Issue: New Trends on Construction Technologies and Sustainable Building Materials

Recent Progress in Materials
2023, volume 5, issue 3
doi:10.21926/rpm.2303029

Received: April 28, 2023
Accepted: July 24, 2023
Published: July 27, 2023

Abstract

In recent years, regional wars and terror activities have caused blast-loading effects on reinforced concrete buildings, resulting in catastrophic human and material damage. When a building is exposed to a blast load, a very high air pressure affects the building within a very short duration. To decide on the reconstruction or retrofit of a building exposed to blast loading, the behavior of the building under blast loading should be investigated. In this paper a case study of a RC building exposed to blast loading during the Libyan war in the last years was investigated. Nonlinear analysis results indicate that the failure mode is localized and that most structural elements remain elastic after explosions. The paper presents, building description details, material tests, finite element model and nonlinear analysis results.

Keywords

Blast; explosion; reinforced concrete; nonlinear analysis; building

1. Introduction

In the last decades, many buildings in the wide world have been subjected to explosions with multiple impacts, resulting in catastrophic human and material damages. Hence building's vulnerability and behavior under these extreme loadings must be investigated. In literature several experimental and analytical works investigate the effect of blast loadings on civil structures and their structural elements. Anas et al. investigate the effect of blast air pressure and its induced ground shock on a masonry heritage building [1]. X. Lin et al. developed a finite element model to simulate the structural response of reinforced concrete panels under blast loading effects. Their study investigated the effect of charge weight, standoff distance, panel thickness and reinforcement ratio on the panel's blast resistance [2]. Yi Xiao et al. tested two full-scale RC arch slabs under contact explosion at and off the bottom center of the mid-span cross-section. They found that the damage was concentrated on the front side surface of the slab and similar to a triangle fully-penetrated area originating from the detonation location to the front side surface of the slab [3]. Jianguo Ning et al. investigated the behavior of concrete slabs subjected to blast loading at different stand-off distances, and a fragment model to predict the fragment degree of a concrete slab subjected to blast loading was established [4]. Aoude et al. investigate blast loads' effect on ultra-high performance fiber reinforced concrete (UHPFRC) columns using a shock-tube [5]. Their results show that using UHPRFC improves the blast performance of RC columns. H.M. Elsanadedy et al. tested RC circular columns subjected to blast loads [6]. Their results show that the maximum lateral deflection experienced by the column decreased exponentially with the increase in stand-off distance. In this paper behavior of a case study reinforced concrete building affected by blast loading during the war activities in 2017, was investigated. The building is located in Benghazi city, Libya and consists of two floors. It is symmetrical about one of its axes and it was constructed in the mid-seventies of the last century. During the war action in the last years, the building was exposed to blast loads which induced architectural and structural damages. The main structural damage was a dismantled collapse of a main column in the second story of the west façade. Furthermore, the building suffered a complete collapse of the staircase roof including its beams and columns, as shown in Figure 1 (i.e. Photos 1.1 to 1.4). The detonation forces affecting the building are dynamic and were modeled as such. These forces are represented as impulse forces as specified in ACI 370 [7]. The authors used different scaled distances to simulate the blast forces that induced the damage with the help of the data given in UFC 3- 340-02 specifications [8]. The structure was modeled using a non-linear finite element model to determine the time history of its response. The nonlinearity in the reinforced concrete beams was modeled using moment-rotation hinges at both beam ends. The hinges' modeling parameters were selected as specified by ASCE 41-17 specification [9]. The nonlinearity in the reinforced concrete columns was modeled by a parametric interactive axial load and moments (i.e., P-M2-M3) hinge at both column ends using the plasticity theory. The hysteresis models apply to different hinges following the Takeda model as described in Takeda, Ozen and Nielsen (1970) [10]. The following sections of this paper present building description details, material properties, nonlinear analysis model, and analysis results.

Figure 1 Structural damages due to blast loadings in the case study building.

2. Description of the Structure

In this case study, the building was constructed in the early seventies and made of in-situ conventional reinforced concrete. It consists of two floors connected by columns and a staircase. The total plan area of each floor is 200 m^2 with a height 3.2 m. Each floor consisted of a 250 mm thick hollow block concrete slab, with ribs spaced at 420 mm, center to center as shown in Figure 2. The ribbed slab is supported on embedded main beams of 800 × 250 mm and 600 × 250 mm reinforced with 8 ϕ 16 top and bottom and 6 ϕ 16 top and bottom, respectively. Both beams are reinforced with stirrups ϕ 8 mm spaced at 150 mm. Beams supported on 200 × 400 columns with 6 ϕ 14 main reinforcement and ϕ 8 mm stirrups spaced at 200 mm.

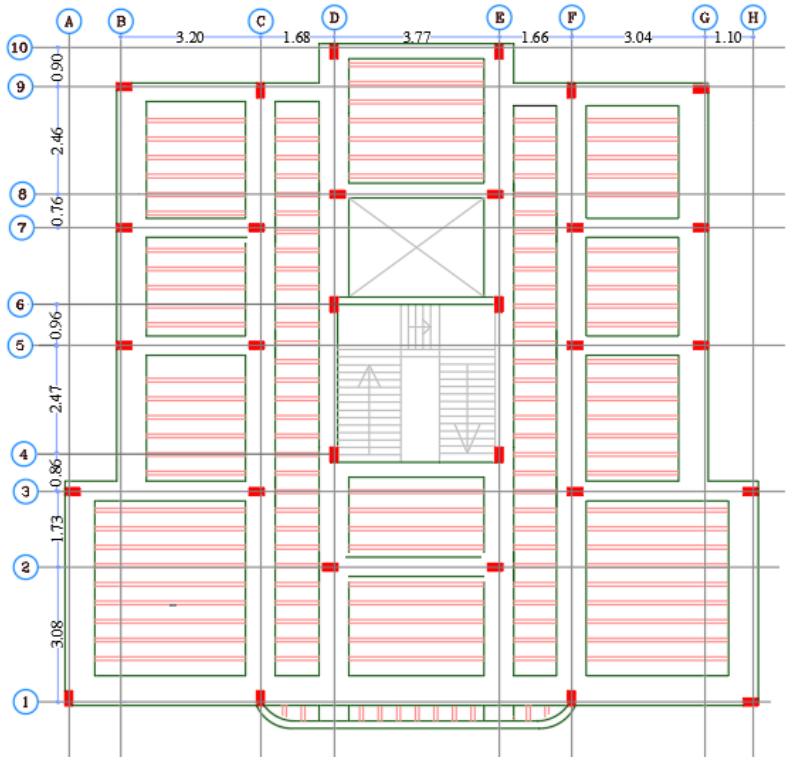

Figure 2 Structural elements of the building, ribbed slab, embedded beams and columns.

The columns were supported on isolated RC square footings 1.5 × 1.5 × 0.5 m at a depth 0.8 m from the existing natural ground level resting on the moderately strong limestone layer.

3. Materials Properties

3.1 Concrete

To investigate the concrete properties of the building, we extracted 12 core samples from the different structural elements of the building as per ASTM C 42. The location of cores was selected based on the results of non-destructive tests and visual inspection. We apply the appropriate strength correction factors for core length-to-diameter ratios less than 2.0. The following properties and concrete parameters shown in Table 1, Table 2, and Table 3 represent the average values estimated from core sample testing.

Table 1 Design properties of concrete.

Compressive Strength of Concrete $f_{c'}$	15.6 Mpa
Direct Tensile Strength of Concrete f_t	1.34 Mpa
Shear Strength v_c	2.69 Mpa

Table 2 Mechanical and design properties of concrete.

Modulus of elasticity, E	18.3 Gpa
Poisson's Ratio, μ	0.15
Shear Modulus, G	8 Gpa

Table 3 Parametric strain data of concrete.

Strain at Maximum Stress, e_o	0.0021 mm/mm
Strain at Failure, e_u	0.003 mm/mm
Strain at Rupture in Tension, e_t	0.00018 mm/mm

3.2 Reinforcing Steel

ASTM A370 permits sampling, laboratory, and destructive testing to determine existing steel bar properties of existing buildings. The yield and tensile strength for reinforcing steels were obtained as per ASTM A370, where a minimum of three sample coupons, are retrieved from the exposed reinforcement. From experimental testing of the rebar samples, the average properties and parameters of the steel reinforcement are summarized in Table 4, Table 5, and Table 6.

Table 4 Design properties of reinforcement steel.

Minimum Yield Stress F_y	350 Mpa
Maximum Tensile Strength F_u	570 Mpa
Expected Yield Stress F_{ye}	318 Mpa
Effective Tensile Strength F_{ue}	518 Mpa

Table 5 Parametric strain data of reinforcement steel.

Strain at Onset of Strain Hardening, e_o	0.013 mm/mm
Strain at Maximum Stress, e_u	0.11 mm/mm
Strain at Rupture, e_r	0.18 mm/mm

Table 6 Mechanical properties of reinforcement steel.

Modulus of Elasticity, E	201 Gpa
Poisson's Ratio, μ	0.3
Shear Modulus, G	77 Gpa

4. Blast Wave Energy

Blast wave energy is a phenomenon that occurs when a large release of energy takes place in an air medium due to detonation. This sudden release of energy leads to a drastic increase in pressure in the medium, giving rise to a pressure disturbance known as a blast wave. The blast wave is a shock wave that propagates outward from the detonation point, with an initial decrease in pressure followed by an overpressure. The shock wave is strongest immediately after the detonation and decreases rapidly as it moves away from the source.

The blast wave has several distinct characteristics: peak overpressure, impulse, and duration. The peak overpressure is the maximum pressure exerted by the blast wave. The duration of the blast wave is the time it takes for the pressure to decay, and is typically measured in milliseconds (ms). The effects of a blast wave on the environment and nearby structures depend on several factors,

such as the size and type of explosive used, the distance from the detonation site, and the nature of the surrounding environment. The larger the explosive and the closer the detonation site, the more significant the damage will be.

A triangular shape is assumed for the dynamic blast load with a sudden rise and linear decay for design purposes. The negative phase, usually following this curve, is neglected because it usually has little effect on the maximum response see Figure 3 and Figure 4. For design purposes, the reflected maximum pressure was idealized by an equivalent triangular pulse of maximum peak pressure P_r and time duration t_d, which yields the reflected impulse I_r,. This generally gives good results particularly if the duration of the applied load is less than the response time of the structural element, ACI 370R-14.

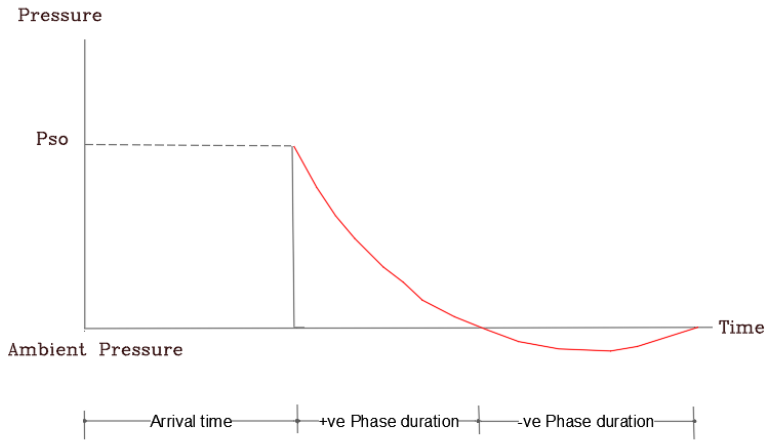

Figure 3 The actual blast load pressure.

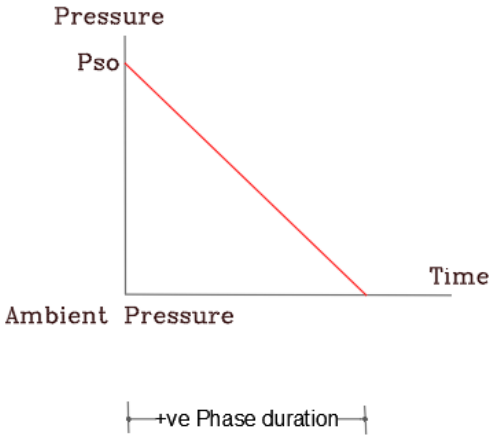

Figure 4 Idealized blast load pressure.

5. Pressure Time History

To evaluate the load time shape on the structural elements, we use the following procedure, first, we calculate the scaled distance $Z = R/(W^{1/3})$. Where R is the distance from the center of the detonation point to the face of the investigated element and W is the weight of the equivalent TNT

explosive. Based on this value, the peak pressure, time of duration, and other parameters can be found in **UFC 3- 340-02**.

We assumed different scaled distances, and found the maximum pressures and impulses affecting the building. The forces due to blast loading were applied to the building as triangular loading functions calculated separately for each joint of the front face of the building, taking into account the distance to each joint from the source of the blast. Reflected overpressure at each joint is multiplied by the tributary area to get the peak load at the Joints. The load time history of each joint and member of the structure can be generated from CSI ETABS 20.

The forces that resulted in the same damage to the building are as specified in Table 7, with the general layout showing the air blast detonation and the locations under investigation as shown in Figure 5.

Table 7 Values of pressure and impulse acting at locations 1 and 2.

Location	Scaled Distance (Z)	Pressure Kpa	Impulse Kpa.ms
1	4	131	3661
2	8.2	118	523

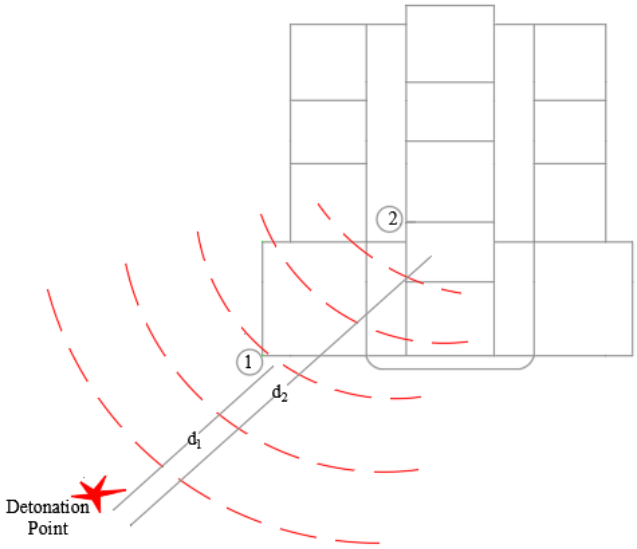

Figure 5 The location of air blast and locations 1 and 2 at distances d_1 and d_2 from detonation point.

6. Modeling of the Structure

The response of a building to blast loading is intricate, since it deals with high-strain rates in the range of 10 to 10^4 s^{-1}, the materials' nonlinear plastic behavior and the structure's time-dependent response.

This paper uses the advantage of CSI ETABS 20, which facilitates using the finite element method with different material properties in the elastic and inelastic zones. Elastic and inelastic properties are input to the program from the results testing of representative samples as shown in section 3. We modeled the RC beams with moment-rotation hinges at both ends for M2 and M3 with the help

of ASCE 41-17 [7] modeling parameters. We modeled the RC columns at both ends with a parametric P-M2-M3 hinge which uses plasticity theory to model P-M2-M3 interaction. The hysteresis models applicable to the different types of hinges follow the Takeda model as described in Takeda, Ozen and Nielsen (1970). The damping ratio for the structure is assumed to be 5% in the dynamic analysis.

7. Structural Response

Figure 6 shows the deformed shape of the building due to blast loading. It also shows the joints that reached the collapse stage (shown in green) and the locations of the investigated structural objects. The collapsed joints in the figure mean that column C2-1, as well as the structural elements of the upper staircase roof have collapsed. This is consistent with the extent of the damage that occurred to the building under the effect of blast forces.

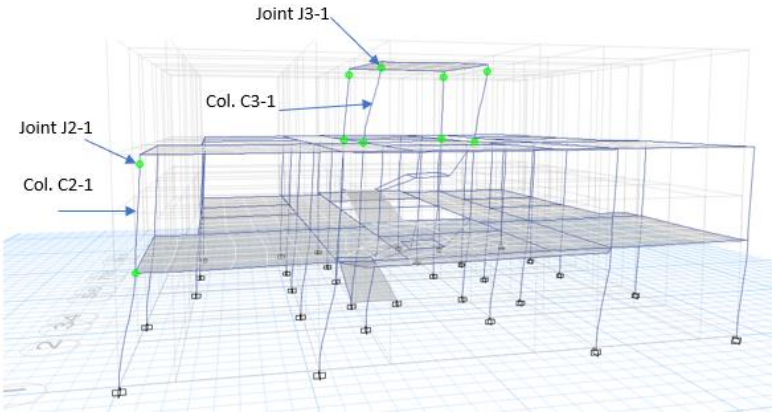

Figure 6 Deformed shape, Plastic joints and Location of investigated objects.

The following figures show the response of different objects of the structure. These objects are shown in Figure 6. Figure 7 shows the displacement, velocity and acceleration variation with time at joint J2-1. Figure 8 shows the displacement, velocity and acceleration variation with time at joint J3-1. Figure 9 shows the variation of bending moment with time of the collapsed columns C2-1 and C3-1.

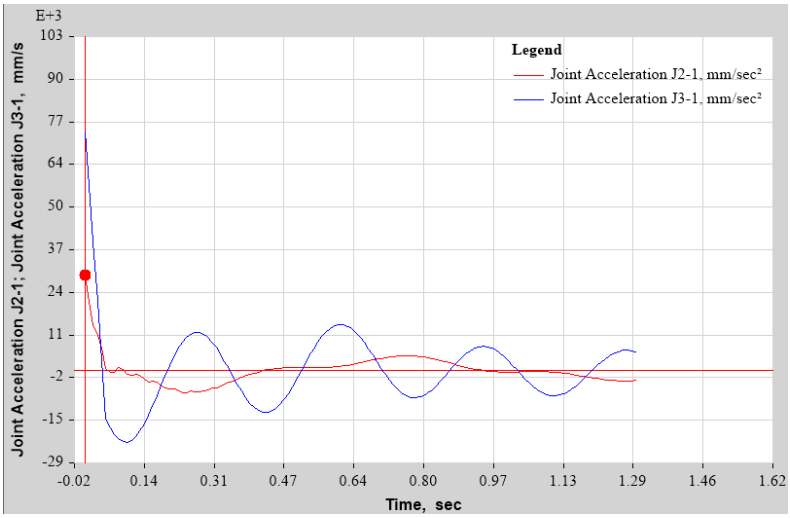

Figure 7 Variation of acceleration with time for joints J2-1 and 3-1.

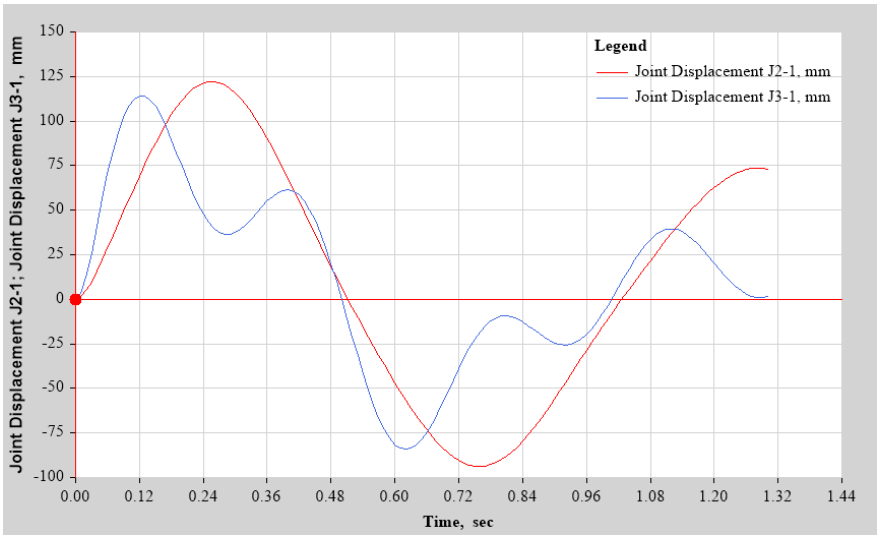

Figure 8 Variation of displacement with time for joints J2-1 and 3-1.

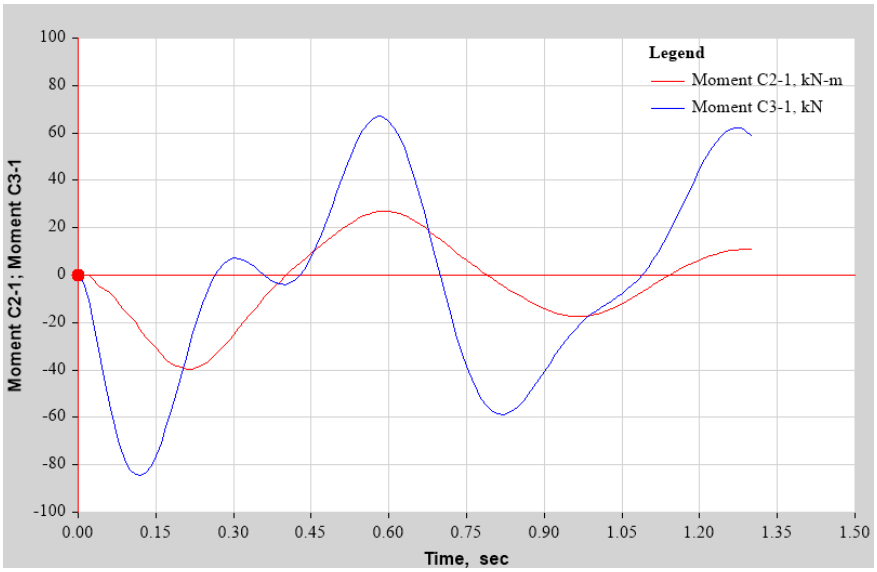

Figure 9 Variation of maximum bending moment with time for columns C2-1 and C3-1.

8. Building Response after Removing Collapsed Objects

To compare the measured in-situ deflection of the first-floor slab and the calculated deflection by the finite element method, we first removed the collapsed objects in the structural model, and after analyzing the structure, we obtained the vertical deflection of the first-floor slab due to the existing gravity loads. This vertical deflection of the slab is shown in Figure 10.

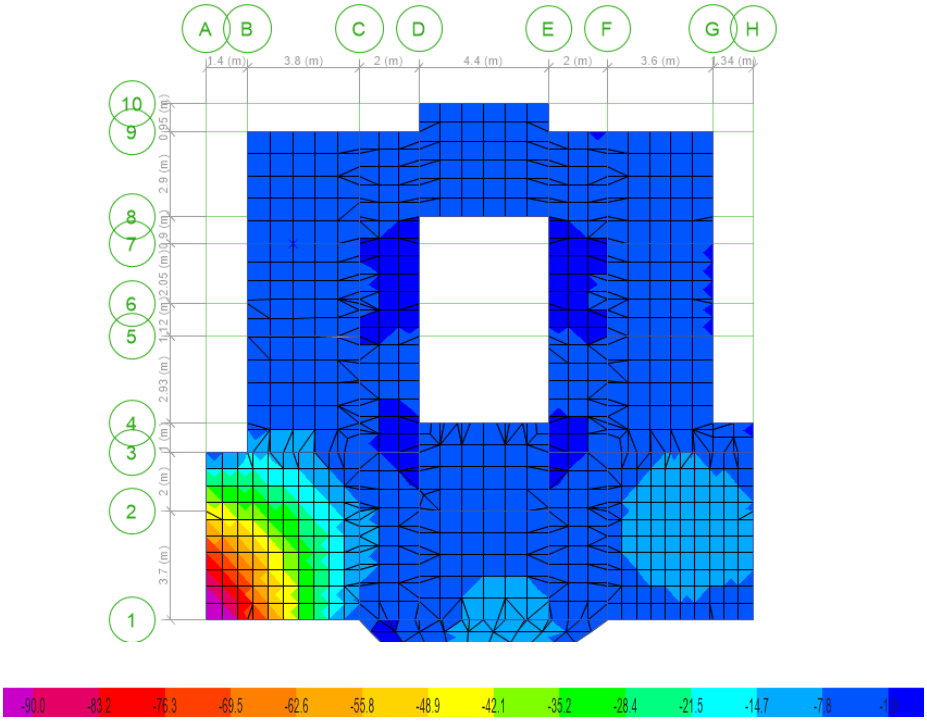

Figure 10 Contour lines of the vertical deflection of the first-floor slab.

Generally, the in-situ vertical deflection of slabs is usually determined by conventional surveying instruments such as total station or geodetic GPS receivers. In this paper, we used the total station type Leica Nova TS60 to measure the vertical deflection of the first floor of the building. The slab face is divided into 6 monitoring points whose coordinates are shown in Table 8. The spatial distribution of these points was located where the maximum deflections are expected in the area of interest.

Table 8 Comparison between the in-situ deflection and FEM solution of the 1st slab.

Point	x(m)	y(m)	Deflection (mm)	
			In-situ	FEM solution
1	0.2	0.2	-89	-90.1
2	2.2	2.2	-34	-34.5
3	7.5	1.8	-7.8	-5.3
4	8.5	4.2	-4	-3.2
5	10.4	0.8	-6	-5.6
6	14.5	3.8	-8	-8.3

Table 8 shows the coordinates of these points and compares the in-situ measured values of the deflection and the finite element solution at these points. We noticed that they compare very well, this confirms that the properties and parameters of the materials used, reasonably, describe the materials of the structure.

9. Conclusions

From the Finite element model, time history analysis results, material tests and site measurements the following conclusions can be withdrawn:

1. The materials properties of the building are below the minimum values set by UFC 3- 340-02 for buildings to be safe against blat loading.
2. The response of the building at joints J2-1 and J3-1 exceeds the limitation set in UFC.
3. After removing the failed objects, the deformed shape produced by the existing gravity loads is similar to that predicted by the elementary theories of elasticity. This means that all the remaining elements are still in the elastic zone. That is failure mode due to localized blast loadings and most structural elements remain elastic after explosions.

As the scaled distance decreases, the blast forces increase. This means blast forces are directly proportional to the explosion material weight and inversely proportional to the standoff distances.

Author Contributions

The 3 authors equally, contributed to this research.

Competing Interests

The authors have declared that no competing interests exist.

References

1. Anas SM, Ansari MI, Alam M. Performance of masonry heritage building under air-blast pressure without and with ground shock. Aust J Struct Eng. 2020; 21: 329-344.
2. Lin X, Zhang YX, Hazell PJ. Modelling the response of reinforced concrete panels under blast loading. Mater Des. 2014; 56: 620-628.
3. Xiao Y, Zhu W, Wu W, Guo P, Xia L. Damage modes and mechanism of RC arch slab under contact explosion at different locations. Int J Impact Eng. 2022; 170: 104360.
4. Ning J, Yang S, Ma T, Xu X. Fragment behavior of concrete slab subjected to blast loading. Eng Fail Anal. 2022; 138: 106370.
5. Aoude H, Dagenais FP, Burrell RP, Saatcioglu M. Behavior of ultra-high performance fiber reinforced concrete columns under blast loading. Int J Impact Eng. 2015; 80: 185-202.
6. Elsanadedy HM, Almusallam TH, Abbas HU, Al-Salloum YA, Alsayed SH. Effect of blast loading on CFRP-Retrofitted RC columns-a numerical study. Lat Am J Solids Struct. 2011; 8: 55-81.
7. ACI. Report for the design of concrete structures for blast effects. Reported by ACI committee 370. Farmington Hills: American Concrete Institute; 2014; ACI 370R-14.
8. Unified Facilities Criteria (UFC). Structures to resist the effects of accidental explosions. U. S. Army Corps of Engineers, Naval Facilities Engineering Command, Air Force Civil Engineer Support Agency; 2008; UFC 3-340-02.
9. ASCE. Design of blast-resistant buildings in petrochemical facilities. Reston, VA: American Society of Civil Engineers; 1997.
10. Takeda T, Sozen MA, Nielsen NN. Reinforced concrete response to simulated earthquakes. J Struct Div. 1970; 96: 2557-2573.